Role of radiolytic oxygen in the x-ray production and thermal annealing of defects in high-purity amorphous SiO_2

Lin Zhang, V. A. Mashkov, and R. G. Leisure
Department of Physics, Colorado State University, Fort Collins, Colorado 80523
(Received 11 September 1995)

Direct experimental evidence for the presence and x-ray dose dependence of radiolytically displaced oxygen in high-purity, oxygen-deficient a-SiO_2 is presented. Anneal-interrupted x-irradiation and electron spin resonance measurements were used to investigate the x-ray dose dependence of the radiation response of two types of low-OH a-SiO_2, i.e., oxygen-excess and oxygen-deficient materials. The production and thermal annealing of paramagnetic defects in these two materials were compared to explore the role played by dissolved and radiolytically displaced oxygen in these processes. The multiple, reversible interconversions of E' centers and peroxy radicals proved to be very sensitive to the presence of free oxygen in the a-SiO_2 network. Such interconversions are very probable in the oxygen-excess material due to the presence of dissolved oxygen. It follows that such interconversions are not expected in the oxygen-deficient material, at least at low dose, in agreement with experimental data. However, our results show that such interconversions take place above a certain threshold dose in oxygen-deficient material. In fact, we observed peroxy radicals in oxygen-deficient material. Their production is attributed to the presence of radiolytically displaced oxygen in this material. A simple physical model is presented to explain the results. The model involves the random creation of displaced oxygen atoms which undergo elastically driven recombination into oxygen molecules. It is these molecules which participate in the interconversions in the oxygen-deficient material. A threshold is observed because the recombination does not occur unless the distance between the oxygen atoms is less than some characteristic length, i.e., a correlation radius of an elastically coherent nanoregion in the amorphous network. The experimental results and the model imply a universal radiation response at high dose when the density of radiolytically displaced oxygen exceeds that of any precursors.

I. INTRODUCTION

High-purity amorphous silicon dioxide (a-SiO_2), prepared as bulk synthetic silica, optical fibers, or thin films, is the most important wide-band-gap material used in modern telecommunications and electronics technologies. It is used in optical waveguides, in gate oxides for metal-oxide-semiconductor (MOS) devices, and in a wide variety of transmissive and reflective optical components. Defects in the as-deposited thin films and in the as-drawn optical fibers, or defects resulting from energetic particle or photon radiation,[1] result in a series of localized energy levels in the energy gap of these materials. Such localized states strongly affect electronic and optical properties due to charge trapping, quantum transitions among the defect levels, and transitions between the defect levels and the conduction- or valence-band states. These defects are intimately related to the long-term reliability of silica-based optical fibers and thin films. It is well documented that radiation-induced defects in bulk a-SiO_2 and fiber-drawing-induced defects in optical fibers are similar, if not identical. The three most important paramagnetic defects in a-SiO_2 are the E' center, the peroxy radical (PR), and the nonbridging-oxygen hole center (NBOHC). The E' center has received extensive study since it was reported by Weeks.[2] It is firmly identified as an unpaired spin of an electron trapped on the dangling sp^3 hybrid orbital of a silicon atom at one side of an asymmetric oxygen vacancy, $\equiv Si\cdot$.[3] The peroxy radical was attributed by Friebele *et al.*[4] to a hole delocalized over a pair of unbonded $2p$ orbitals on *two* oxygen atoms in a bonded oxygen molecule, though preferentially localized on the terminal one, $\equiv Si—O—O\cdot$. The nonbridging-oxygen hole center, has been assigned by Stapelbroek *et al.*[5] to a hole trapped on an unbonded $2p$ orbital of a nonbridging oxygen atom, $\equiv Si—O\cdot$. (The symbol $\equiv Si$ represents a silicon atom bonded to three oxygens in the glass network and a dot stands for an unpaired spin.) Several diamagnetic defects resulting from the manufacturing process, such as neutral oxygen vacancies ($\equiv Si—Si\equiv$), peroxy linkages ($\equiv Si—O—O—Si\equiv$), strained or broken Si—O bonds, and hydroxyl groups ($\equiv Si—OH$), can serve as precursors for the above-mentioned paramagnetic defects. For instance, the tension associated with fiber drawing can break a Si—Si bond and make an E' center,[6] i.e., a mechanically induced atomic rearrangement. However, the formation of observable paramagnetic point defects by such a mechanical process must be accompanied by a redistribution of electrons and holes in the network, i.e., by ionization. In contrast, the initial step in radiation-induced defect production is the ionization of the valence bands and the preexisting defect structures in the network. The corresponding atomic rearrangement is a secondary effect. The fact that there is no apparent difference between radiation-induced and fiber-drawing-induced defects indicates that the defect structures are strongly coupled vibronic systems whose response is independent of the type of perturbation. However, the probability of an induced atomic transformation into a defect structure is clearly dependent on the type of perturbation.

The radiation response of a-SiO_2 is strongly dependent on the concentration of abnormal bonds, i.e., the deviation of the system from the perfect continuous random network. Among the most common sources of abnormal bonds are nonstoichiometric oxygen content, OH and Cl impurities, and thermal history (fictive temperature).[7] Keeping in mind the close connection between defects in bulk silica and optical fibers, in this paper we consider the role of oxygen in defect production and annealing in bulk a-SiO_2. The role of oxygen has been studied previously by several workers. Stapelbroek and co-workers[5] studied Suprasil W1, which is a low-OH, oxygen-excess material.[8] They found that annealing the irradiated material in the temperature range of 100–200 °C resulted in the growth of the peroxy radical concentration with a concomitant decay of the E' center concentration. Edwards and Fowler[9] suggested that this conversion was due to the trapping of dissolved oxygen molecules at the E' center sites to form peroxy radicals:

$$E' + O_2 \Rightarrow \mathrm{PR}. \tag{1}$$

By running experiments on samples with controlled O_2 content, Pfeffer[10] demonstrated the role of dissolved O_2 in the above reaction. Recently,[11] using repeated irradiation-anneal experiments, we reported the reverse of reaction (1) and demonstrated multiple interconversions of the E' center and the PR in Suprasil W1,

$$E' + O_2 \Leftrightarrow \mathrm{PR}. \tag{2}$$

Given the crucial role attributed to oxygen in reaction (2), it seems important to study the production, and possible interconversion, of defects in *oxygen-deficient* material. We report such studies in the present paper and compare the results to those for oxygen-excess material. We irradiate these two types of materials with known doses of x rays. The resulting defects are investigated using electron spin resonance (ESR). We find that the defect production efficiency and dose dependence differ strongly for these two types of materials. As expected, no interconversions of the type described by reaction (2) are observed at low to moderate doses in the oxygen-deficient material. However, interconversions *are* observed at high dose. We attribute such interconversions to radiolytic oxygen and give a theoretical description of the results. We also deduce a critical radius for the diffusion-limited combination of radiolytic oxygen atoms into oxygen molecules.

II. EXPERIMENTAL DETAILS

All experiments were carried out on two types of bulk samples of ''dry'' silica (OH content less than 2 ppm) with different oxygen contents. Suprasil W1 has about 10^{18} cm^{-3} excess oxygen molecules.[10] This excess oxygen is assumed to be in the form of interstitial oxygen molecules and peroxy linkages Si—O—O—Si. The oxygen-deficient samples used here, designated J8 in the present paper, have about 10^{17} cm^{-3} Si—Si bonds as measured by optical absorption.[12] In preparation for the experiments, the materials were cut into rectangular samples: the dimensions of the oxygen-deficient samples were $35\times6.5\times1$ mm^3, and the dimensions of the oxygen-excess samples were $10\times3\times1$ mm^3. All samples were etched with 48% HF acid to remove any impurities on the surface. The samples were x irradiated at a volume-average dose rate of $q=1.5$ Mrad/h. The GE x-ray machine with a W tube was operated at 45 kV and 20 mA. The x rays were incident normally on the large face of the samples. The penetration depth of the most intense x rays was much greater than the 1 mm thickness of the samples. After one-half of each irradiation cycle, the sample was reversed in the x-ray beam and then irradiated from the opposite face. As a result the dose profile in each sample was determined to be uniform within 25%. Except where noted, the irradiation was performed at room temperature. In a few cases, samples of oxygen-deficient material were irradiated at 77 K to investigate radiolytic hydrogen and chlorine. Following irradiation, the samples were stored in liquid nitrogen when not in the ESR spectrometer. The spectrometer used was a Bruker ESP 300 spectrometer with a temperature controller. The spectrometer was operated at X-band frequency (9.47 GHz). First-derivative spectra were obtained using 100-kHz modulation frequency under nonsaturating conditions. Absolute spin densities were determined to an accuracy of about 50% by a comparison method. The spin standard was a 1.0 mM toluene solution of the stable nitroxyl radical tempone, whose geometrical shape was similar to that of our samples. The ESR spectra of the E' centers were measured at room temperature while the spectra for the oxygen hole centers were recorded at 100 K in order to resolve the lines of the NBOHC and the peroxy radical.

Two types of experiments were performed. In the first type of experiment, the concentration of various spin-active defects was determined by irradiating the samples to a known accumulated dose, removing the samples from the x-ray beam to record the ESR spectra, and then repeating this procedure to acquire a concentration vs dose curve for the various defects. In the second type of experiment, the above concentration vs dose curve was interrupted with a thermal anneal, and then the concentration vs dose curve continued. Several consecutive radiation-anneal cycles were studied. The experimental procedures were described in more detail previously.[11]

III. EXPERIMENTAL RESULTS

A. Defect production

Several variants of the E' center are known,[13,14] and the most common is the E'_γ center. Figure 1 shows the E'_γ concentration $[E'_\gamma]$ versus accumulated dose (Mrad SiO_2) for these two materials in the uninterrupted irradiation experiments. The open symbols and closed symbols represent, respectively, the oxygen-excess and the oxygen-deficient materials. Over the entire dose range investigated, $[E'_\gamma]$ increased sublinearly with dose in both materials, and E'_γ centers were created *more efficiently* in oxygen-deficient material than in oxygen-excess material.

The sample dependence of the oxygen hole center concentration (Fig. 2) was opposite to that of $[E'_\gamma]$, i.e., fewer oxygen hole centers were detected in oxygen-deficient material than in oxygen-excess material. The dose dependence also differed from that of $[E'_\gamma]$. As Fig. 2 shows, the dose dependence of the oxygen hole center concentration is sublinear in the oxygen-excess material while it is linear or su-

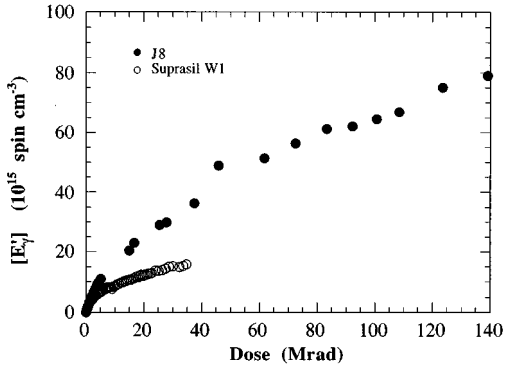

FIG. 1. E'_γ spin concentration vs accumulated x-ray dose obtained from room-temperature ESR measurements on two samples of low-[OH] a-SiO_2: Suprasil W1, an oxygen-excess material, and J8, an oxygen-deficient material. The samples were x irradiated at room temperature.

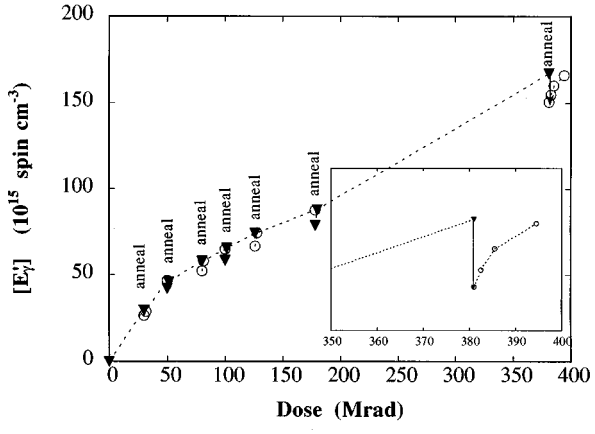

FIG. 3. E'_γ spin density versus x-ray dose in the anneal-interrupted irradiation experiments on oxygen-deficient material. At the points indicated, the irradiation was interrupted with a soft anneal (225 °C, 10 min). The inset shows the detail of the seventh cycle.

pralinear in the oxygen-deficient material. It is important to note that only the NBOHC was observed in the oxygen-deficient samples. The oxygen hole center signal in oxygen-excess material contains contributions from both NBOHC's and peroxy radicals. Figure 2 shows the total oxygen hole center concentration. The ratio of the concentrations of E'_γ centers to oxygen hole centers was about 40 in the oxygen-deficient material, but only about 4 in the oxygen-excess material.

In addition to the E'_γ and the NBOHC, two additional defects were observed in the oxygen-deficient material: the E'_δ center, i.e., a variant of the E' center, and a triplet state.[14–18] These two centers have about the same dose dependence, namely, saturating with x-ray dose easily (at about 1–5 Mrad). These defects will not be discussed in the present paper, but will be presented in a future publication.

B. Defect annealing

In thermal-anneal-interrupted irradiation experiments, the experiments described above are interrupted with a thermal anneal, and then the measurement of defect concentration versus dose is continued. We previously described such experiments on oxygen-excess material (Suprasil W1).[11] Those experiments showed that a soft thermal anneal (225 °C for 10 min) was sufficient to erase completely the E' signal. Concomitant with the decrease of the E' concentration, the PR concentration increased. The NBOHC concentration did not change with the soft anneal. Upon resuming the irradiation, the PR concentration decreased rapidly while the E' center concentration showed a corresponding increase. We previously interpreted these effects as due to the interconversion of E' centers and PR's by means of molecule oxygen.

According to the above discussion, the results for the oxygen-deficient material should differ strongly from those for the oxygen-excess material. Indeed, we find a strong difference between these two materials. Figure 3 shows the results for the E'_γ center. An anneal of 10 min at 225 °C causes only minor changes in $[E'_\gamma]$ especially at doses below 50 Mrad. Such an anneal was sufficient to erase completely the E'_γ center in the oxygen-excess material. In marked contrast, an anneal of 1 h at 800 °C is required to completely erase the E' center in the oxygen-deficient material. As Fig. 3 shows, however, the soft anneal does produce some decrease in $[E'_\gamma]$, and this decrease becomes more significant at higher dose. This effect will be discussed in more detail below. Figure 4 shows the effect of the soft anneal on the NBOHC concentration. As can be seen, there is a large effect. Figure

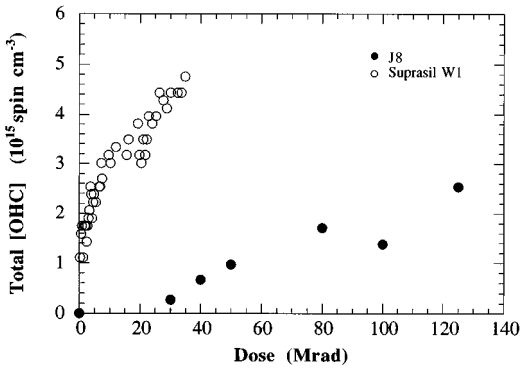

FIG. 2. Total oxygen hole center concentration for the samples of Fig. 1. The ESR measurements were performed at 77 K.

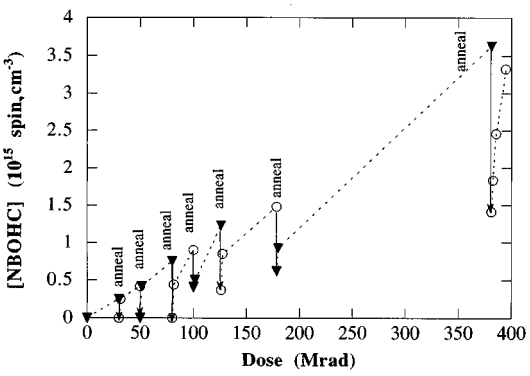

FIG. 4. The NBOHC spin density versus x-ray dose for oxygen-deficient material for the same conditions as in Fig. 3.

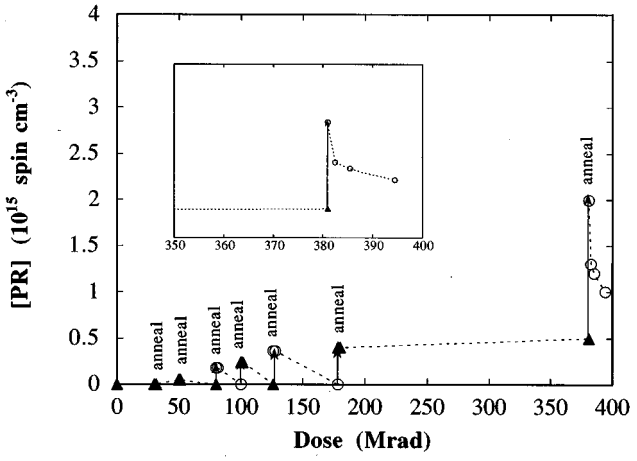

FIG. 5. The peroxy radical spin density versus x-ray dose for oxygen-deficient material for the same conditions as in Fig. 3.

5 shows the effect of the soft anneal on the PR concentration. Below about 50 Mrad *no peroxy radicals are observed*. Such a result is in marked contrast to the situation for the oxygen-excess material where such an anneal produced a strong increase in the PR concentration. According to the model described by reaction (2), PR's were not expected for the oxygen-deficient material. However, starting at about 80 Mrad, *peroxy radicals appear upon annealing* and the thermally produced PR concentration increases rapidly with dose. More details are shown in Fig. 6 for an oxygen-deficient material irradiated to 400 Mrad. Before the soft anneal, the low-temperature (100 K) oxygen hole center ESR spectrum shows only the nonbridging-oxygen hole center without peroxy radicals. However, upon annealing, peroxy radicals dramatically appear. The postanneal irradiation bleached some of the peroxy radicals created during the soft anneal.

Tsai and Griscom[19] previously presented experimental evidence for the presence of radiolytic oxygen in high-purity silicas, i.e., Suprasil 1 and 2, which contain stoichiometric network oxygen and about $10^{19}/\mathrm{cm}^3$ OH groups. The origin of the radiolytic oxygen was attributed to network oxygen due to the exciton decay mechanism. However, due to the high concentration of OH groups, the radiolytic production of oxygen from this latter source cannot be ruled out. In the present work, peroxy radicals have been observed in low-OH, oxygen-deficient materials. The only possible origin of these centers appears to be radiolytic oxygen *from the network*. In that sense, the present work represent the most direct experimental evidence for the radiolytic creation of oxygen from the network.

At extremely high doses the concentration of radiolytic oxygen is likely to exceed that of any precursors. In this regime the radiation hardness is expected to have a universal behavior, independent of precursors. Griscom[20] has recently reported the radiation hardening of optical fibers at ultrahigh doses to processes involving radiolytic oxygen.

An additional effect was observed in the interrupted anneal experiments on the ''dry,'' oxygen-deficient materials. The soft anneal converted about 90% of the remaining E'_γ ESR signal to the E'_β-like line shape. The conversion of E'_γ centers into E'_β centers upon annealing was observed previously by Griscom[13] in high-OH a-SiO_2. The present work shows that this effect is reversible, i.e., the E'_β centers convert into E'_γ centers upon resumption of irradiation.

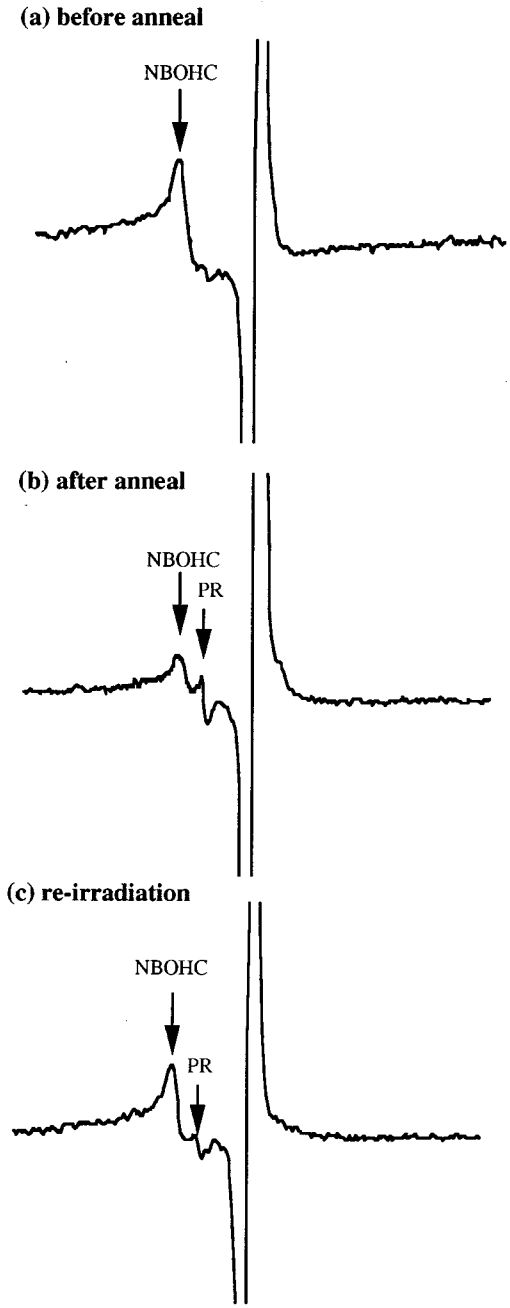

FIG. 6. ESR spectra showing details of the anneal and post-anneal irradiation behavior for an oxygen-deficient sample which had been irradiated to 400 Mrad. The spectra were recorded at 77 K.

C. Other defects produced by low-temperature irradiation

We observed ESR signals due to atomic H^0 and Cl^0 signals in both Suprasil W1 and J8 after x irradiation at 77 K. The ESR signals were measured at the same temperature. The samples were kept in liquid-nitrogen continuously when

TABLE I. Defect yields in oxygen-deficient (J8) and oxygen-excess (Suprasil W1) low-[OH] silicas as determined by ESR measurements. Samples were x irradiated to 5 Mrad and the ESR measurements performed at 77 K immediately following the irradiation. The H^0 and Cl^0 measurements were made on samples x irradiated at 77 K; other measurements were carried out on samples irradiated at room temperature. N.D. indicates "not determined."

	Defect concentration (10^{15}/cm^3)						
Sample	$[E'_\gamma]$	[NBOHC]	[PR]	$[H^0]$	$[Cl^0]$	$[E'_\delta]$	[Triplet]
Suprasil W1[a]	5.15	1.08	2.52	0.72	1.62	N.D.	N.D.
J8[b]	12.60	0.2	N.D.	0.15	6.13	0.7	0.15

[a]Manufactured by Haraeus-Amersil.

[b]Provided by Dr. H. Hosono of Tokyo Institute of Technology.

they were transferred from the x-ray machine to the ESR spectrometer, since these two signals were thermally very unstable and annealed out at room temperature. These two signals were characterized by Griscom and Friebele.[14,21,22] They showed that H^0 and Cl^0 diffuse rapidly to dimerize with other H^0 or Cl^0 and convert to molecular H_2 and Cl_2 at about 130 and 300 K, respectively. The origin of the radiolytic H^0 and Cl^0 can be attributed to dissociation of Si—OH, Si—H, and Si—Cl bonds. The spin concentrations of the two centers at 5 Mrad dose are listed in Table I along with the concentration of other paramagnetic defects. As can be seen, there are significant differences of $[H^0]$ and $[Cl^0]$ in the two materials.

IV. DISCUSSION

A. Comparison of detect production in oxygen-excess and oxygen-deficient materials

Figures 1 and 2 show that E' center generation is more efficient in the oxygen-deficient material as compared to the oxygen-excess material, while the reverse holds true for oxygen hole center generation. One contribution to the generation of E' centers and NBOHC's in both materials is presumably the fissure of, perhaps strained, Si—O—Si bonds,

$$2(\equiv\text{Si—O—Si}\equiv)+h\nu\rightarrow(\equiv\text{Si—O}\cdot\ ^{+}\text{Si}\equiv)+(\equiv\text{Si—O}^{-}\cdot\text{Si}\equiv). \quad (3)$$

The energy $h\nu$ in reaction (3) is supplied by the secondary electrons resulting from the x-ray absorption. In order to account for the different efficiencies for defect generation in the two materials shown in Figs. 1 and 2, it is necessary to examine the role played by precursors and oxygen-associated defect conversion.

The higher number of E' centers in the oxygen-deficient material can be accounted for qualitatively in terms of the higher number of precursors in this material. These precursors are associated with the oxygen deficiency and with impurities. The oxygen deficiency in sample J8 results in a large number (10^{17}cm^{-3}) of Si—Si homobonds. These act as precursors for E' generation according to

$$\equiv\text{Si—Si}\equiv+h\nu\rightarrow\equiv\text{Si}\cdot+\ ^{+}\text{Si}\equiv+e^{-}. \quad (4)$$

Other precursors may include Si—Cl and Si—H bonds. Under radiation, E' centers can be formed by radiolysis of those bonds,

$$\equiv\text{Si—H}+h\nu\rightarrow\equiv\text{Si}\cdot+\text{H}^0 \quad (5)$$

and

$$\equiv\text{Si—Cl}+h\nu\rightarrow\equiv\text{Si}\cdot+\text{Cl}^0. \quad (6)$$

Table I shows that a relatively large Cl^0 concentration was observed in the oxygen-deficient material following low-temperature irradiation; the H^0 concentration was lower in both materials, but larger in the oxygen-excess material as compared to the oxygen-deficient material. Thus, reactions (5) and especially (6) probably also contribute to a larger E' concentration in the oxygen-deficient material as compared to the oxygen-excess material.

As discussed above, it has been shown that E' centers may convert rapidly to PR's in oxygen-excess material at temperatures of about 200 °C. It seems likely that this process also occurs at room temperature, although at a reduced rate. We have also shown that, under room-temperature irradiation, some of these PR's reconvert to E' centers. It seems plausible that during the room-temperature irradiation of the oxygen-excess material reaction (2) leads to a net production of PR's and thus accounts for the larger oxygen hole center production in the oxygen-excess material as compared to the oxygen-deficient material.

B. E'-PR interconversion in oxygen-deficient material

The interconversion of E' centers and PR's observed in oxygen-excess material[11] is not expected in low-OH, oxygen-deficient material due to the lack of the interstitial molecular oxygen. Indeed, such interconversions are not observed at low dose in the oxygen-deficient material, indicating the absence of O_2 molecules. However, starting at about 80 Mrad accumulated dose in the oxygen-deficient material such interconversions are observed; and, as Figs. 3 and 5 show, the magnitude of the effect increases strongly with dose. This interconversion implies that radiolytic oxygen molecules are present in the irradiated, oxygen-deficient material, and their concentration increases sharply with dose.

We propose a simple physical model to explain this unusual behavior of oxygen in irradiated, low-OH, oxygen-deficient material. Our explanation is based on the fact that glass (silica glass, in particular) is a strongly disordered system which can be characterized on average by a correlation length R_c. The existence of such a correlation length has been well documented with a number of experimental techniques and theoretical approaches.[23] However, the numerical

value of R_c is strongly dependent on the nature of the physical phenomenon under consideration. For example, the correlation length for intermediate-range order in amorphous silica (from x-ray diffraction data) is about 40 Å.[24] The correlation length for processes of transport and scattering of charged carriers (free electrons and holes) in silica is quite different. In this paper, with regard to the problem of soft annealing in irradiated oxygen-deficient silica, we will be interested in yet a different correlation length which characterizes a space relaxation of elastic strain, stress, and interatomic interactions associated with radiation-induced point defects in glass.

The concept of a correlation length allows us to consider amorphous silica as a disordered system consisting of a set of nanoregions of different sizes and shapes that fill out the entire sample, and behave as coherently self-connected elastic microregions. The mean size of these nanoregions is designated by the quantity R_c. This characteristic scale plays an essential role for our further consideration.

As is well known, amorphous silica tends toward compaction under irradiation. Radiation-induced compaction might be explained in part by a strong attractive interaction between radiolytically displayed oxygen atoms because the volume of an O_2 molecule is less than the volume of two separated oxygen atoms in silica, $V(O_2)<2V(O)$. However, this attractive interaction (which would be a long-range elastic attraction in a crystal lattice) is cut off at the correlation radius R_c in the case of a disordered glass network. Thus this interaction between oxygen atoms can be considered as an analogue of the screened Coulomb (or Yukawa) potential.

In accordance with the concept of a correlation length R_c, we have independent diffusion of oxygen atoms in different nanoregions if the mean distance between them exceeds the correlation length for the elastic interaction, $R>R_c$. We assume that, within a nanoregion, the driftlike motion dominates the diffusive motion. With this assumption, if at least two oxygen atoms are generated in one nanoregion, $R\leqslant R_c$, they always combine into an O_2 molecule with probability 1.

To demonstrate the existence of R_c and to obtain a rough estimate of its value, we proceed as follows. We use the results in Figs. 1 and 5 to plot the change in [PR] on annealing vs the average separation of E' centers. The average separation of E' centers at a particular dose is just proportional to $[E']^{-1/3}$. The results are presented in Fig. 7. We expect the concentration of E' centers to be proportional to the concentration of radiolytic oxygen atoms at high dose. With this assumption, Fig. 7 shows that the annealing-induced change in [PR] depends very strongly on the average separation of oxygen molecules.

We now present the details of the model. Radiolytic oxygen atoms are created randomly in a-SiO_2 during irradiation. A fraction of these atoms combine into oxygen molecules and participate in the conversion of E' centers into PR's during a subsequent anneal [see Eq. (1)]. We describe the PR and E' concentrations during this time interval by the equations

$$\frac{d[E']}{dt}=-(c_1+c_2)[E'], \quad \frac{d[\mathrm{PR}]}{dt}=c_1[E']. \tag{7}$$

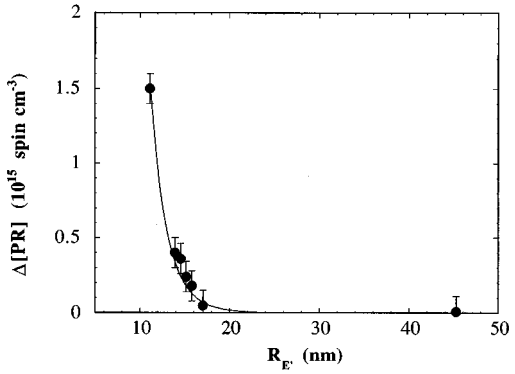

FIG. 7. Thermal-anneal-induced change in PR concentration vs $R_{E'}$ for the oxygen-deficient material. The solid line represents the theoretical expression discussed in the text.

We assume first that both c_1 and c_2 are constant, and we further assume that $c_1=L[O_2]$ where L is a constant. Solving these equations shows that the *change* in the PR concentration during the anneal is given by

$$\Delta[\mathrm{PR}]=K[E'][O_2], \tag{8}$$

where K is a constant which depends on L, c_2, and the annealing time, and $[E']$ is the E' concentration at the *beginning* of the anneal. Equation (8) is the solution of the kinetic problem stated by Eqs. (7) above; it is not a rate equation nor does it represent a mass action law; it is simply the net change in PR concentration during the thermal anneal. The preceding discussion was based on a constant c_1. In fact $[O_2]$, and hence c_1, probably depends on time. Two cases may be treated: O_2 molecules may be created during the irradiation and consumed in reaction (1) during the anneal; and O_2 molecules may be created *and* consumed during the anneal. In either situation, $[O_2]$ as a function of time probably has a well-defined maximum. In such conditions, a step-function approximation for the time dependence of $[O_2]$ allows us to simplify the integration of the rate Eqs. (7) with a time-dependent c_1, and get Eq. (8) as a result. In this case $[O_2]$ in Eq. (8) represents the time-averaged value of $[O_2]$ during the anneal. The constant K in this case depends on L, c_2, the annealing time, and the shape function describing the time dependence of $[O_2]$.

The concentration of E' centers appearing in Eq. (8) is determined directly from the ESR data. We now proceed to estimate the concentration of O_2 using the concept of a nanoregion discussed above. The nearest-neighbor distribution function $G(R)$ for the case of randomly distributed defects is[25]

$$G(R)=4\pi R^2 N_0 \exp\left(-\frac{4\pi}{3}R^3 N_0\right), \tag{9}$$

where N_0 is the density of defects, which in the present case we take to be the density of radiolytically displaced oxygen atoms. The probability of the recombination of O atoms into O_2 molecules is proportional to the integral of $G(R)$ over a nanoregion so that

$$[O_2]=\tfrac{1}{2}N_0\int_0^{R_c}dRG(R)=\tfrac{1}{2}N_0\left[1-\exp\left(-\frac{4\pi}{3}R_c^3N_0\right)\right]. \tag{10}$$

As discussed above, we assume that, at high dose, $N_0=\alpha[E']$, where α is somewhat less than unity (see below). If we define $R_{E'}$ as the mean separation of E' centers before the thermal anneal ($[E']=(4\pi R_{E'}^3/3)^{-1}$), the resulting theoretical formula for the data of Fig. 7 is given by the expression

$$\Delta[\mathrm{PR}]=\frac{1}{2}K\alpha\left(\frac{4\pi}{3}R_{E'}^3\right)^{-2}\left\{1-\exp\left[-\alpha\left(\frac{R_c}{R_{E'}}\right)^3\right]\right\}. \tag{11}$$

The solid line in Fig. 7 is a fit of Eq. (11) to the data with the value of $\alpha^{1/3}R_c=16$ nm and $K\alpha=10^{-19}$ cm^3. As can be seen, the equation gives a good description of the sharp increase in the anneal-induced PR concentration at high dose. The actual values of the fitting parameters should be viewed with caution for several reasons. Because of the limited range of the $R_{E'}$ for which we have nonzero values of [PR], the results are rather insensitive to the value of R_c used in Eq. (11). In addition, all parameters are renormalized by the parameter α. This renormalization is not so serious for R_c, because α only enters as the cube root. However, a value of 16 nm is in the range of the size of nanoregions which might be expected in a-SiO_2. If we take $\alpha\approx 1/10$, then we see that $K^{1/3}\approx 10$ nm. Interpreting this later value in terms of Eq. (8), we might expect that 10 nm represents a capture radius for the reaction of an E' center with an O_2 molecule during the whole soft thermal annealing process. The results appear self-consistent.

We can place a lower limit on the parameter α by the following argument. Comparing Figs. 3 and 5 shows that the *increase* in PR concentration during annealing is approximately 1/80 times the E' concentration. This increase is a measure of the minimum concentration of O_2 molecules and leads to $\alpha\geqslant 1/40$. In fact, we may assume that the total atomic oxygen concentration is at least a few times greater than this value; thus the value of 1/10 used seems reasonable.

The mechanism based on dimerization of oxygen presented above gives a good account of our results. As a possible alternative mechanism, radiolytic oxygen might convert E' centers to PR during annealing by the two reactions

$$E'+\mathrm{O}\Rightarrow\mathrm{NBOHC} \tag{12a}$$

and

$$\mathrm{NBOHC}+\mathrm{O}\Rightarrow\mathrm{PR}. \tag{12b}$$

Figures 3 and 4 show that the concentration of E' centers is roughly two orders of magnitude greater than that of NBOHC. Under this condition, reaction (12a) should occur at a much higher rate than reaction (12b) during the thermal anneal, leading to an initial *increase* of the NBOHC concentration. However, Fig. 4 shows that the NBOHC concentration *decreases*. In addition, the various isochronal annealing studies in the literature always show a decrease of the NBOHC concentration. Thus reactions (12) do not appear to play an important role in thermal annealing. A comparison of Figs. 4 and 5 provides additional evidence that reactions (12) do not make a significant contribution in the present case. The annealing of NBOHC shows a smooth behavior as a function of dose, while the annealing of the PR's shows an onset at about 80 Mrad. Thus these two oxygen hole centers appear to anneal by different processes.

C. Other annealing mechanisms

Our previous results[11] on the interconversion of E' centers and PR's in oxygen-excess material showed that there was not a one-to-one correspondence between the decrease in $[E']$ and the increase in [PR] on annealing for 10 min at 225 °C; the decrease in $[E']$ was greater than the increase in [PR]. In the case of oxygen-deficient material, a close inspection of Figs. 3 and 5 shows that a similar relation holds. In addition, as Fig. 4 shows, the [NBOHC] decreases on annealing in the oxygen-deficient material. (The soft anneal also removes the E'_δ center and triplet states discussed earlier.) These facts strongly suggest that there must be effective annealing mechanisms at 225 °C other than that of oxygen-diffusion-limited reactions. At such moderate temperatures, the predominant annealing mechanisms may be controlled by the diffusion of small interstitial molecules.

It is well known that chlorine is a fairly common impurity in synthetic SiO_2.[26,27] Some silicas contain high concentrations (>4000 ppm) of chlorine, which come from the manufacturing process such as dehydration from silica soot boules and plasma oxidation of $SiCl_4$. Table I shows, for the special case of irradiation and ESR measurement at 77 K, a relatively large concentration of Cl^0. In the oxygen-deficient material the total concentration of this atomic chlorine is about one-half the concentration of the E'_γ centers. These atoms are probably produced radiolytically from Si—Cl bonds as indicated by reaction (6). It seems likely that Cl_2^- is also produced during the low-temperature irradiation due to trapping of electrons released by reaction (4), although this species normally would not be observable by ESR (see, however, Ref. 1). It is known that, following irradiation at 77 K, the Cl^0 population decreases rapidly with increasing temperature between 100 and 300 K.[14] This decrease is probably due to the diffusion-controlled dimerization of atomic chlorine. Given the large number of Si—Si homobonds present in the oxygen-deficient material and the relatively high Cl^0 population produced by low-temperature irradiation, it seems likely that the predominant sources of E'_γ centers are reactions (4) and (6) during both low-temperature and room-temperature irradiation. Considering the mobility of Cl^0 at room temperature and the large number of electrons released by reaction (4), it seems likely that the radiolytic chlorine resulting from room-temperature irradiation will be mostly in the form of Cl_2^- with a relatively small population of Cl_2^0. Both the Cl_2^- and the Cl_2^0 are expected to be immobile and stable at room temperature.[14,27] At 225 °C, however, the neutral molecules could diffuse and react with the E' centers to produce diamagnetic centers:

$$2(\equiv\mathrm{Si}\cdot)+Cl_2^0\rightarrow 2(\equiv\mathrm{Si—Cl}). \tag{13}$$

The Cl_2^- are more stable than their neutral counterparts; thus they remain immobile in the network until the temperature is raised high enough (>600 °C) to detrap the electrons from the molecular ions, at which temperature they can participate in annealing.

This additional contribution to E'_γ annihilation explains why, during the thermal anneal, the decrease in $[E'_\gamma]$ is greater than the increase in [PR]. For the oxygen-deficient material in the low-dose range, the annealing of E'_γ centers is likely due mainly to molecular chlorine. Since the concentration of NBOHC's is 40 times lower than that of E'_γ centers, similarly, the anneal of NBOHC's may be through the process

$$2(\equiv\text{Si—O}\cdot)+\text{Cl}_2{}^0\rightarrow 2(\equiv\text{Si—OCl}). \qquad (14)$$

V. CONCLUSIONS

We have studied two types of low-[OH] amorphous silica, oxygen excess and oxygen deficient, to investigate the role of nonstoichiometric oxygen concentration in x-ray-induced defect production and thermal annealing. The most interesting feature in the oxygen-excess material is the interconversion of E'_γ centers and PR's. Molecular oxygen plays a key role in this process. Interconversions are also observed in the oxygen-deficient material at high x-ray dose. The observation of E'_γ-PR interconversion in oxygen-deficient silica is direct experimental evidence for the presence of radiolytically displaced oxygen in this material. These interconversions in the oxygen-deficient material increase strongly above a certain threshold dose. A simple physical model is presented to explain the results. Radiolytic oxygen atoms undergo elastically driven recombination into O_2 molecules if their separation is less than a correlation length which corresponds to the mean radius of some elastically coherent nanoregion. The model provides a reasonable description of the experimental results; the best estimate of the correlation radius is 16 nm.

The oxygen-deficient material appears to contain a large number of precursors for E'_γ production, probably due to Si—Si bonds (oxygen vacancies) and Cl impurities. These precursors account for the higher efficiency of E'_γ production in the oxygen-deficient material, while interconversion may account for the higher efficiency of oxygen hole center production in the oxygen-excess material for the dose range investigated. The present results on the role of radiolytic oxygen imply that at very high dose, when the density of radiolytic oxygen exceeds that of any precursors, the radiation response may be a universal feature, independent of the type of silica.

ACKNOWLEDGMENTS

This work was supported by the Office of Naval Research under Contract No. N00014-91-J-1607. It is a pleasure to thank D. L. Griscom for many valuable comments and suggestions. We are grateful to H. Hosono for the oxygen-deficient material and stimulating discussions.

[1] D. L. Griscom, J. Ceram. Soc. Jpn. **99**, 923 (1991), and references therein.
[2] R. A. Weeks, J. Appl. Phys. **27**, 1376 (1956).
[3] F. J. Feigl, W. B. Fowler, and K. L. Yip, Solid State Commun. **14**, 225 (1974).
[4] E. J. Friebele, D. L. Griscom, M. Stapelbroek, and R. A. Weeks, Phys. Rev. Lett. **42**, 1346 (1979).
[5] M. Stapelbroek, D. L. Griscom, E. J. Friebele, and G. H. Sigel, Jr., J. Non-Cryst. Solids **32**, 313 (1979).
[6] H. Hanafusa, Y. Hibino, and F. Yamamoto, J. Appl. Phys. **58**, 1356 (1985).
[7] F. L. Galeener, D. B. Kerwin, A. J. Miller, and J. C. Mikkelsen, Jr., Phys. Rev. B **47**, 7760 (1993).
[8] Haraeus-Amersil, 3473 Satellite Blvd., Duluth, GA 30316.
[9] A. H. Edwards and W. B. Fowler, Phys. Rev. B **26**, 6649 (1982).
[10] R. L. Pfeffer, in *The Physics and Technology of Amorphous SiO_2*, edited by R. A. B. Devine (Plenum, New York, 1988), p. 181.
[11] Lin Zhang, V. A. Mashkov, and R. G. Leisure, Phys. Rev. Lett. **74**, 1605 (1995).
[12] H. Hosono (private communication).
[13] D. L. Griscom, Nucl. Instrum. Methods Phys. Res. Sect. B **1**, 481 (1984).
[14] D. L. Griscom and E. J. Friebele, Phys. Rev. B **34**, 7524 (1986).
[15] K. Vanheusden and A. Stesmans, J. Appl. Phys. **74**, 275 (1993).
[16] M. E. Zvanut, T. L. Chen, R. E. Stahlbush, E. S. Steigerwait, and G. A. Brown, J. Appl. Phys. **77**, 4329 (1995).
[17] R. A. B. Devine, W. L. Warren, J. B. Xu, I. H. Wilson, P. Paillet, and J. L. Leray, J. Appl. Phys. **77**, 175 (1995).
[18] R. Tohmon, Y. Shimogaichi, Y. Tsuta, S. Munekuni, Y. Ohki, Y. Hama, and K. Nagasawa, Phys. Rev. B **41**, 7258 (1990).
[19] T. E. Tsai and D. L. Griscom, Phys. Rev. Lett. **67**, 2517 (1991).
[20] D. L. Griscom, J. Appl. Phys. **77**, 5008 (1995).
[21] D. L. Griscom, J. Non-Cryst. Solids **73**, 51 (1985).
[22] D. L. Griscom, M. Stapelbroek, and E. J. Friebele, J. Chem. Phys. **78**, 1638 (1983).
[23] *Amorphous Insulators*, edited by M. F. Thorpe and A. C. Wright (North-Holland, Amsterdam, 1995).
[24] R. L. Mozzi and B. E. Warren, J. Appl. Crystallogr. **2**, 164 (1969).
[25] F. Williams, Phys. Status Solidi **25**, 493 (1968).
[26] R. Bruckner, J. Non-Cryst. Solids **5**, 123 (1970).
[27] E. J. Friebele, in *Optical Properties of Glass*, edited by D. R. Uhlmann and N. J. Kriedl (The American Ceramic Society, Westerville, OH, 1991), p. 235.